5-2019

Effect of Thiols for Nitrogen Reduction to Ammonia

Zakary R. Ford
University of Arkansas, Fayetteville

Effect of Thiols for Nitrogen Reduction to Ammonia

Zakary R. Ford[1]

Abstract

Ammonia is an important chemical used for fertilizers and also a potential carbon-free hydrogen storage medium. The Haber-Bosch process is the main production process, which requires large energy- and capital-input. Therefore, it is crucial to develop an alternate scalable synthesis that provides a less energy intensive and more economical route for synthetic ammonia production. In this paper, a 1Fe1Ni film was functionalized with C_3OH and C_6OH for the electrochemical synthesis of ammonia. This work will provide some insight on how thiol ligands can increase the selectivity of the catalyst for nitrogen reduction reaction and can be improved on to provide a new synthesis for ammonia.

[1]University of Arkansas, Ralph E. Martin Department of Chemical Engineering, Fayettville, AR, USA.
Zakary Ford's research was supported by a University of Arkansas Honors College Research Grant.

1. Introduction

With more than 200 million metric tons produced in 2013, ammonia production has increased by 12.5% since 1997 becoming one of the most produced chemicals in the world [1-4]. Ammonia is mainly used to produce artificial fertilizers (80% of total amount produced), which has contributed to human population growth on Earth. The other 20% is used for synthetic chemicals for cleaning agents, dyes, and plastics [1,3]. Besides its uses in fertilizer and synthetic chemical production, ammonia has shown promise to be a cheap and safe substitute for hydrogen in fuel cell technology because of its ease of transportation and storage [1-3]. Three typical pathways for nitrogen fixation exist: catalyzed by nitrogenase, the Haber-Bosch process, and electrocatalysis (Fig. 1) [1].

Out of the three pathways, synthetic ammonia is almost exclusively produced by the Haber-Bosch process which was developed over one hundred years ago by Fritz Haber and Carl Bosch. The Haber-Bosch process relies on highly-concentrated streams of nitrogen and hydrogen at high pressure (150-300 bar) and temperature (400 -500 ºC) to be reacted over iron catalysts to form ammonia with the following reaction [4-7]:

$$N_2 + 3H_2 \rightarrow 2NH_3 \qquad (1)$$

Although the thermodynamics of equation 1 suggests ammonia synthesis is favored at lower temperatures (ΔrH_{300} = -46.35 kJ mol^{-1}) [7], the harsh conditions are required to overcome the sluggish kinetics, a consequence of high nitrogen dissociation energy ($E_{(N\equiv N)}$ = 941 kJ mol^{-1}) [5]. This inevitably connects ammonia synthesis to a large annual energy consumption of over 1% of the total global primary energy supply. In addition, the H_2 used in the reaction is produced via the steam reforming process generating large amounts of "greenhouse" gases (CO_2 is the most abundant) in the range of 300 million metric tons [8-9]. Furthermore, large economies are

required to satisfy the need of the substantial infrastructure of the Haber-Bosch process, which hinders developing countries from producing their own ammonia [8-9].

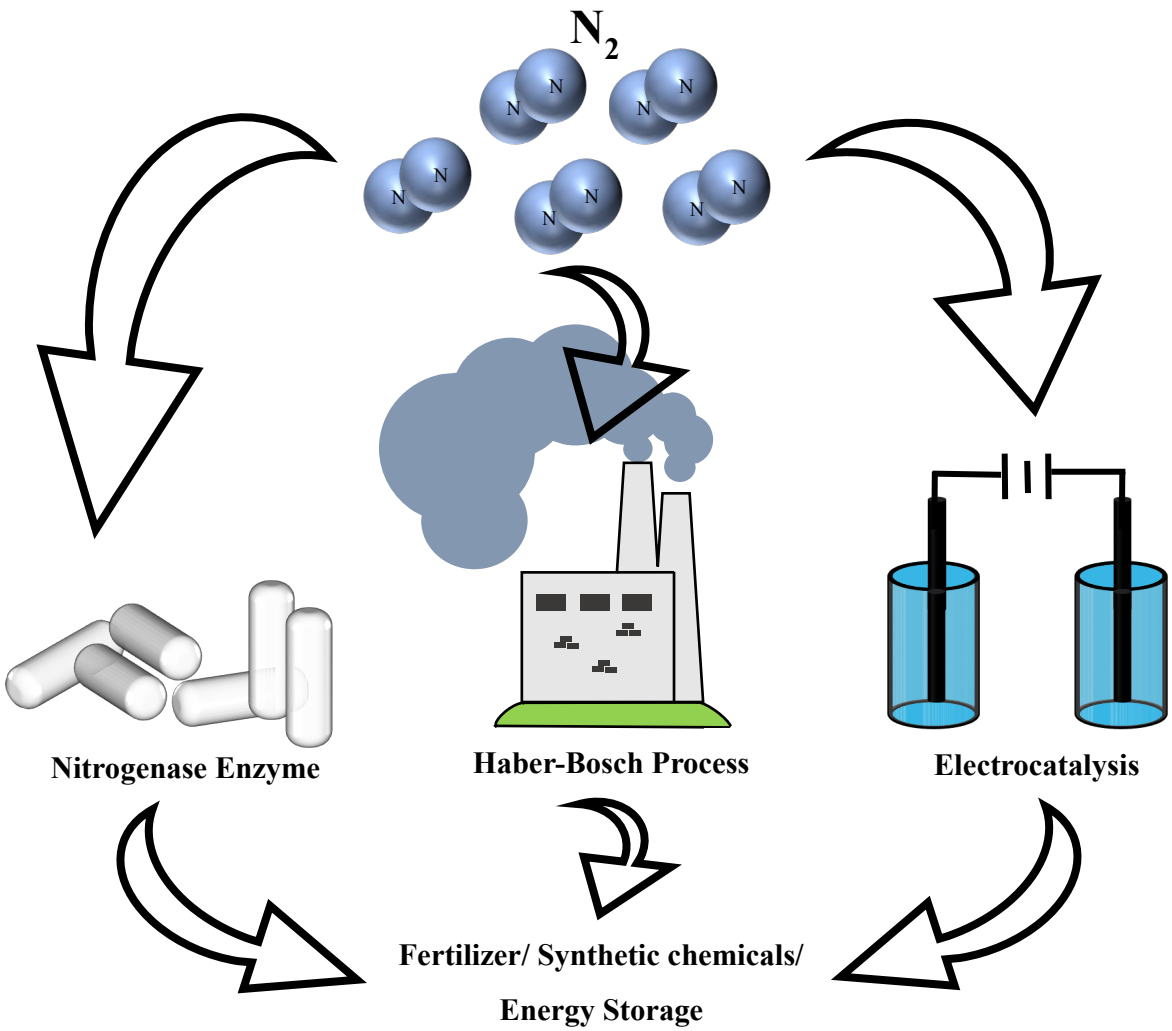

Figure 1. A representation of the three pathways for nitrogen fixation. The products can be used for fertilizer, synthetic chemicals, or energy storage.

Now, this current scenario of ammonia production has garnered research efforts of scientist to pursue a milder route of ammonia production, such as mimicking the enzyme nitrogenase [10-13] or using electrochemical systems [14-17]. For instance, structural and electronic characterization of Mo(HIPTN$_3$N) showed same catalytic functions as the enzyme nitrogenase [18]. Alternatively, photochemical reduction has been reported to produce NH_3 from

N_2 in a chalcogel system of double-cubane and single-cubane [16]. However, many drawbacks still exist with the reported methods, including low yields and slow kinetics [1,3,14].

Another approach is the electrocatalytic N_2 reduction reaction to NH_3 in low-temperature and low-pressure systems, ideally powered by renewable energies (e.g. hydroelectric or geothermal). N_2 molecules can come directly from the air and the protons can be produced by oxidizing water. Electrons would be driven to the surface of the catalyst by applying a potential to the system. This possible solution has enormous potential to impact the energy and environmental sustainability of the production of NH_3 for fertilizers and hydrogen carries. However, the faradaic efficiency of the N_2 reduction reaction are generally low, typically only a few percent [1,3]. Maximum ammonia production rates are also low, on the order of 10^{-8} mol cm^{-2} s^{-1} [1,3,14]. These results are due to the major side reaction of the N_2 reduction reaction (NRR). Hydrogen evolution reaction (HER), in which water is reduced to H_2 gas, in most cases dominates over the NRR. Currently, scientists have been exhaustively studying the catalysts used in the NRR to be able to overcome the strong nitrogen triple bond energy requirement and push the reaction to favor NRR over HER [1-3,14].

To add to this collection of research, the present study focuses on the transition metal complexes based on iron nanoparticles. It has been shown that iron nanoparticles can reduce nitrogen to ammonia at room temperature and ambient pressure [1,2,15,16]. Little is known about the mechanism of this process and in most cases hydrogen evolution dominates over nitrogen reduction to ammonia. In 2012, Skùlason provided insight into optimal catalyst surfaces by performing density function theory (DFT) calculations of ammonia production on flat and stepped surfaces. Analysis of their DFT data suggests that iron will have significant overpotential for nitrogen reduction. As the electrochemical reduction of nitrogen also suffers from selectivity

issues, the result is consistent with experimental observations of iron showing low activity at low temperatures.

The above analysis suggests there must be alternatives in how to design the electrocatalysts for electrochemical nitrogen reduction. Recent progress of N_2 reduction has focused on Fe systems with P and N ligands; however, imitating the sulfur donors of the nitrogenase enzyme have shown promise in catalyst design [19]. Additionally, thiols were used to create a selective surface on Pd/Al_2O_3 catalysts for hydrogenation reactions. The research showed that high sulfur loading was shown to prevent the adsorption of H_2 on the surface of the catalyst. Reaction selectivity was found to be controlled by the sulfur atom while the carbon chain length dictated the catalyst activity [20]. This research suggest that a thiol ligand may be used to control the surface selectivity for electrochemical reactions. By absorbing 3-mercapto-1-propanol (C_3OH), and 6-mercapto-1-hexanol (C_6OH) to iron films through physisorption, the role of sulfur and carbon chain length of thiols in the selectivity of the reaction can be observed.

Furthermore, the DFT analysis suggests that a bimetallic catalyst consisting of elements from either side of the volcano plot may provide a more optimized surface [17]. With this concept in mind, a Fe-Ni nanocomposite will replace the pure iron catalysts. This change in return will increase the current density leading to an increase in ammonia production. However, a decrease in Faradaic efficiency is expected [21,22]. In conclusion, I propose thiol functionalized Fe-Ni based catalysts will mimic the nitrogenase FeMo cofactor function of controlling access of water to the surface of the catalysts and will improve NH_3/H_2 surface selectivity, thus, enhancing the rate of ammonia production.

2. Experimental

The following procedure lays out the experimental foundation used to evaluate the roles of thiol ligand structure and thiol surface loading on water access to the catalyst surface and catalyst selectivity for NH_3. For this approach, two different commercially-available thiols, C_3OH and C_6OH, were used based on their organic chain structure. The thiols were attached to the catalyst through a physisorption method. Based on previous trials in the laboratory, the most successful catalyst tested had a 1:1 ratio of Fe to Ni composition.

Electrochemical studies were carried out using a VSP-300 potentiostat (BioLogic) in a three-electrode liquid electrochemical cell (Fig. 2). A quartz crystal microbalance (QCM) by Biolin Scientific was used to measure the mass response of the working electrode (WE).

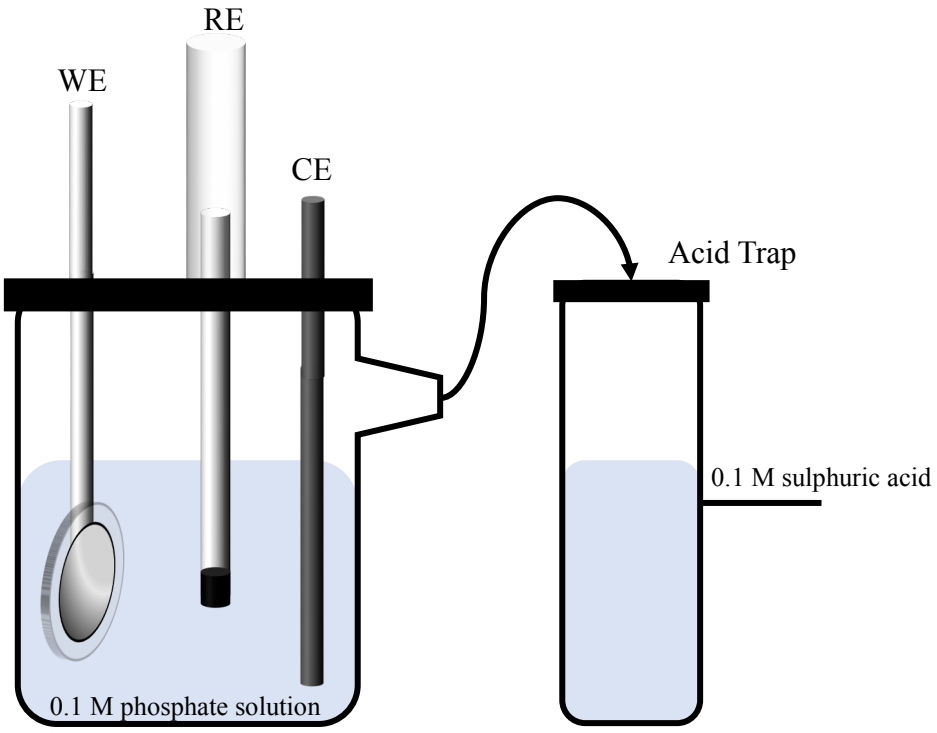

Figure 2. A representation of the three-electrode liquid electrochemical cell. The produced ammonia would be trapped in sulphuric acid in the acid trap.

The commercial WE, an Au quartz crystal wafer (5 MHz, 14 mm diameter) was purchased from Quartz Pro. A carbon rod was used as a counter electrode (CE). A silver-silver chloride electrode immersed in a salt bridge filled with 3 M NaCl was used as the reference electrode. All potentials are reported with respect to this reference electrode. Ultrapure water was used for the preparation of all aqueous solutions. A phosphate buffer solution with no saline was used as the electrolyte. All glassware used in this paper was cleaned by 10% H_2SO_4 solution.

Before the experiments, the Au crystal electrode was first prepared by following the protocol outlined in section 6.1 until stable QCM frequency response was obtained. A Fe-Ni layer was electroplated on the Au electrode in a solution of 0.1 M total metal content of $FeSO_4$ and $NiSO_4$ with and unpublished technique developed by Sergio I. Perez Bakovic in the Greenlee research team. Iron-nickel film coverage was checked by the QCM. Then a 0.1 M thiol solution was flowed over the electrode while still in the QCM. Thiol ligand absorption was determined using the QCM. After rinsing the electrochemical cell with water, degassed electrolyte with nitrogen was introduced. All experiments were performed under ambient temperature and pressure.

Ammonia quantification was done using the indophenol blue method and spectrophotometric analysis. The concentration of indophenol blue was determined using the absorbance at a wavelength of 660 nm and the concentration of ammonia was calculated from a calibration curve prepared by using standard ammonium chloride with a series of concentrations.

3. Results and discussion

3.1 film thickness and thiol loading

QCM was used as the primary source of loading analysis. The QCM allows for quick in situ mass analysis to asses both the film thickness and the total loading of C_3OH and C_6OH onto

the surface of the film. The Sauerbrey equation can calculated film mass as it is related to the mechanical resonance frequency change as shown in equation 2:

$$\Delta f = -C_f \times \Delta m \qquad (2)$$

where Δf is the change in mechanical resonance frequency before and after film deposition, C_f is the sensitivity factor of the 5 MHZ quartz crystal wafer, and Δm is the mass change per area. C_f was defined to be 6.6729 that was calculated by $\frac{2{f_o}^2}{A\sqrt{\rho_q \mu_q}}$ where f_o is the resonant frequency of the crystal wafer, A is the active area of the piezoelectrical crystal, ρ_q is the density of the quartz, and μ_q is the shear modulus of the crystal. Uniform thickness across the quartz crystal was assumed to use the Sauerbrey equation.

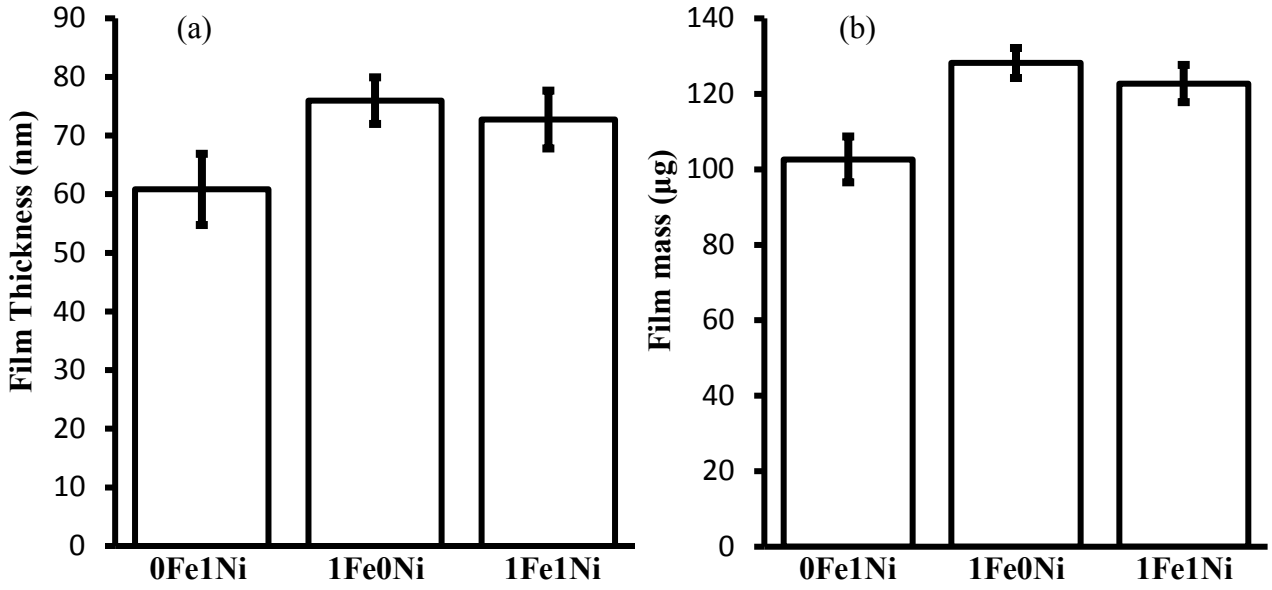

Figure 3. (a) A bar graph showing the film thickness (nm) of each film. (b) A bar graph showing the mass (µg) of each film.

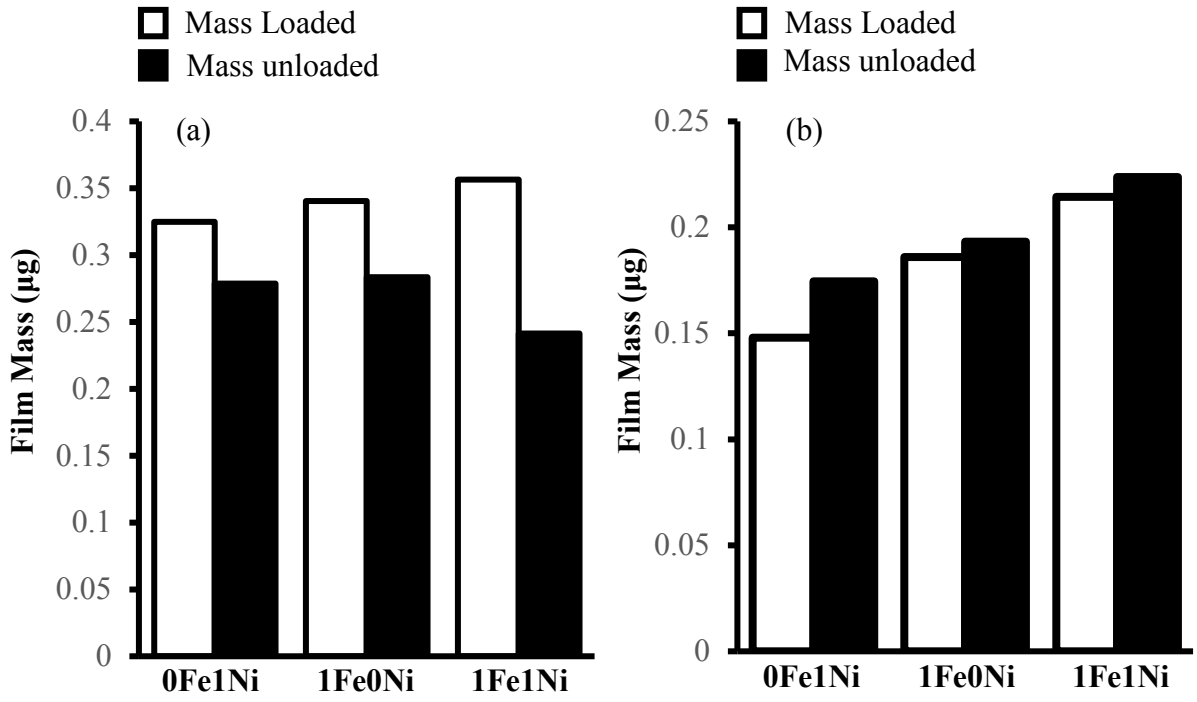

Figure 4. (a) A bar graph showing the mass loading of C_6OH before and after ethanol flow. (b) A bar graph showing the mass loading of C_3OH before and after ethanol flow.

The resulting film thickness and mass change over the Au quartz crystal are show in Figure 3a. Assuming a density of 5.24 g cm^{-3}, as well as the Sauerbrey equation holding, the overall frequency change corresponds to a film thickness of 102.6, 128.2 and 122.7 nm for 0Fe1Ni, 1Fe0Ni, and 1Fe1Ni, respectively. To calculate the film thickness the mass of the films were first calculated and plotted in Figure 3b.

Thiol mass loading of C_3OH and C_6OH were also analyzed using QCM. As Figure 4a and 4b illustrate there was absorption of C_6OH and C_3OH in the range between 0.325 to 0.356 µg and 0.148 to 0.214 µg, respectively. The maximum absorption for both thiols occurred with the 1Fe1Ni film and the minimum with the pure nickel film. This absorption trend illustrates thiols have a higher affinity for Fe and for better absorption higher iron to nickel ratios could be used.

To test the stability of the thiols on the surface of the films, ethanol was flowed over the films while in the QCM. The thiol mass unloaded is show in Figure 4a and 4b as well. There was stable attachment with the C_6OH on each film composition, 1Fe1Ni showed the most promise with 0.115 μg still absorbed to the surface after ethanol flow. As for C_3OH, the mass after ethanol flow was found to be less than the mass before. This mass loss could be explained from some of the film being washed away with the C_3OH. In other words, there was no C_3OH absorbed to the film during the electrochemical analysis.

3.2 ammonia production and determination

In the process of electrocatalysis, N_2 gas and Ar gas were continuously fed to the electrochemical cell, and cyclic voltammetry (CV) tests were performed in Ar- and N_2- saturated 0.1 M phosphate solution between .205 and -0.935 V (vs. RHE). The CV curves (Fig. 5) were different in N_2 and Ar. The NRR is initiated at -0.6 V under N_2-saturated solution, and the current density in N_2-saturated solution is slightly higher than that in Ar-saturated solution, indicating that the 1Fe1Ni film functionalized with C_6OH can effectively catalyze the nitrogen reduction reaction at the potentials range of between -0.6 V and -0.935 V. The same analogous trend is seen with the 1Fe1Ni films functionalized with C_3OH (Fig. 6). However, the CV curve for Ar-saturated solution has some anomalies caused by bubble on the working electrode.

The NRR performance of both films were further estimated by chronoamperometry tests. The chronoamperometry curves in N_2- and Ar- saturated solutions are displayed in Figure 7 & 8. Each curve of the films in different saturated solutions indicate the current density mostly remains constant, indicating their stability for NRR. After electrolysis, concentrations of produced NH_3 in phosphate solution and acid trap were detected by the UV/Vis spectrophotometer.

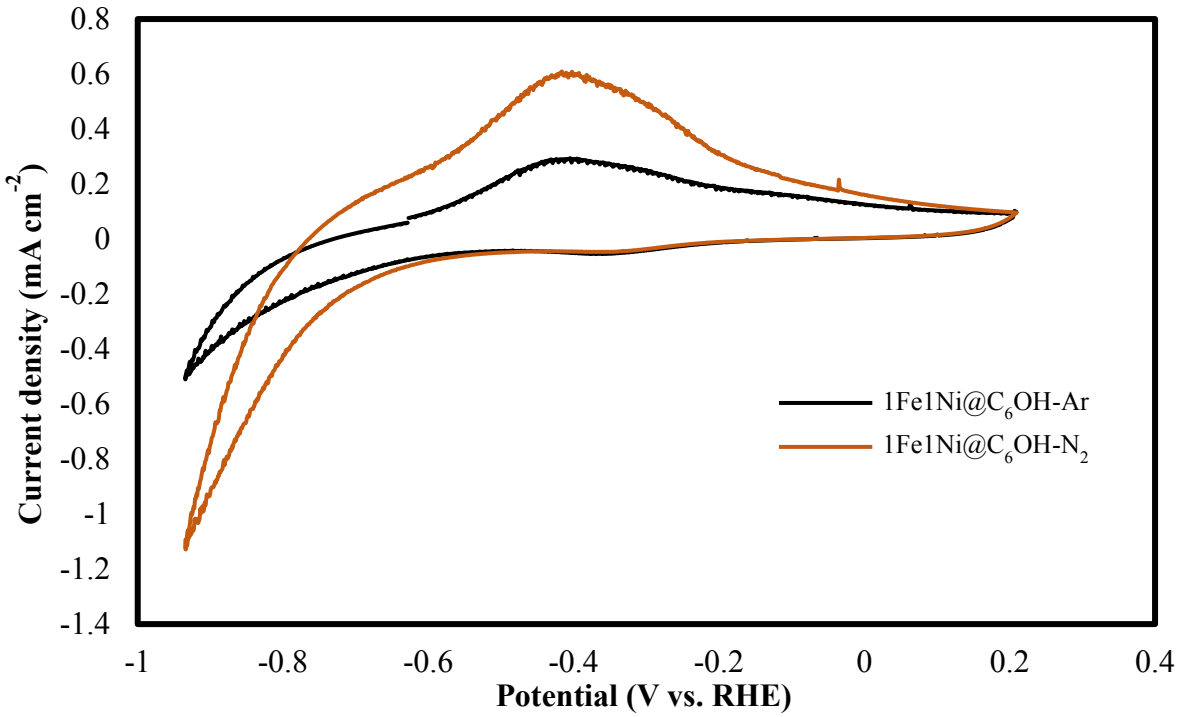

Figure 5. Fifth cycle of CVs collected at 20 mV s^{-1} in 0.1 M phosphate solution for 1Fe1Ni functionalized with C_6OH.

The NH_3 yield and faradaic efficiency (FE) of the different films are calculated and plotted in Figure 9. The yield and FE decreased with the change in the thiol from C_6OH to C_3OH, with maximum values of 41.3 μg h^{-1} $mg_{cat.}^{-1}$ and 6.20%, respectively. FE and ammonia yield of C_3OH were both negative indicating no ammonia was produced and were overwhelmed by the competitive hydrogen reaction. The yield and FE have a significant decrease when analyzing the phosphate solution, which could be explained by the counter electrode oxidizing the produce ammonia in the solution. This performance of the films show promise in NRR and could be improved to be comparable or better than reported catalysts.

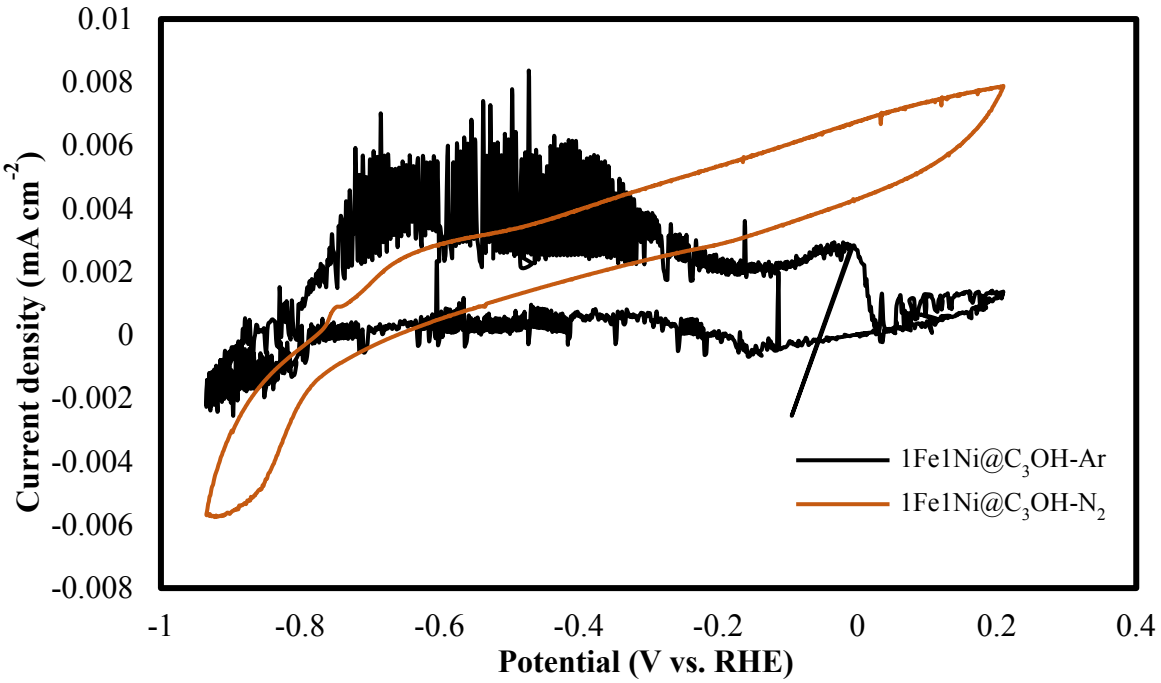

Figure 6. Fifth cycle of CVs collected at 20 mV s^{-1} in 0.1 M phosphate solution for 1Fe1Ni functionalized with C_3OH.

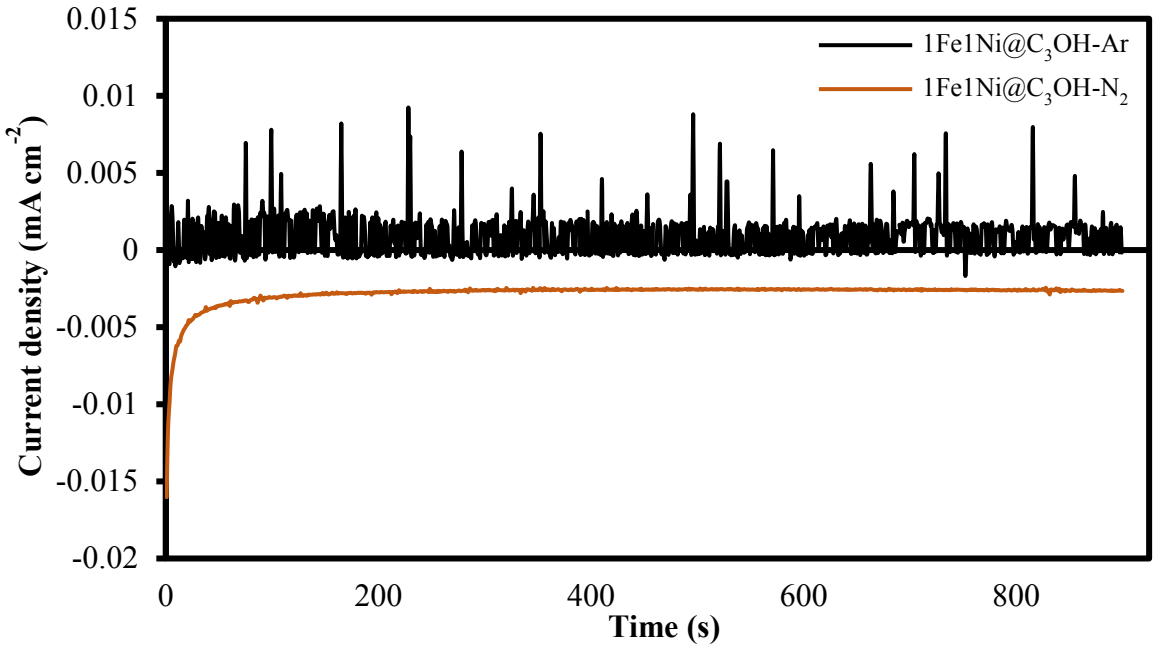

Figure 7. Chronoamperogram of 1Fe1Ni C_3OH functionalized films in 0.1 M phosphate solution under a nitrogen and argon atmosphere.

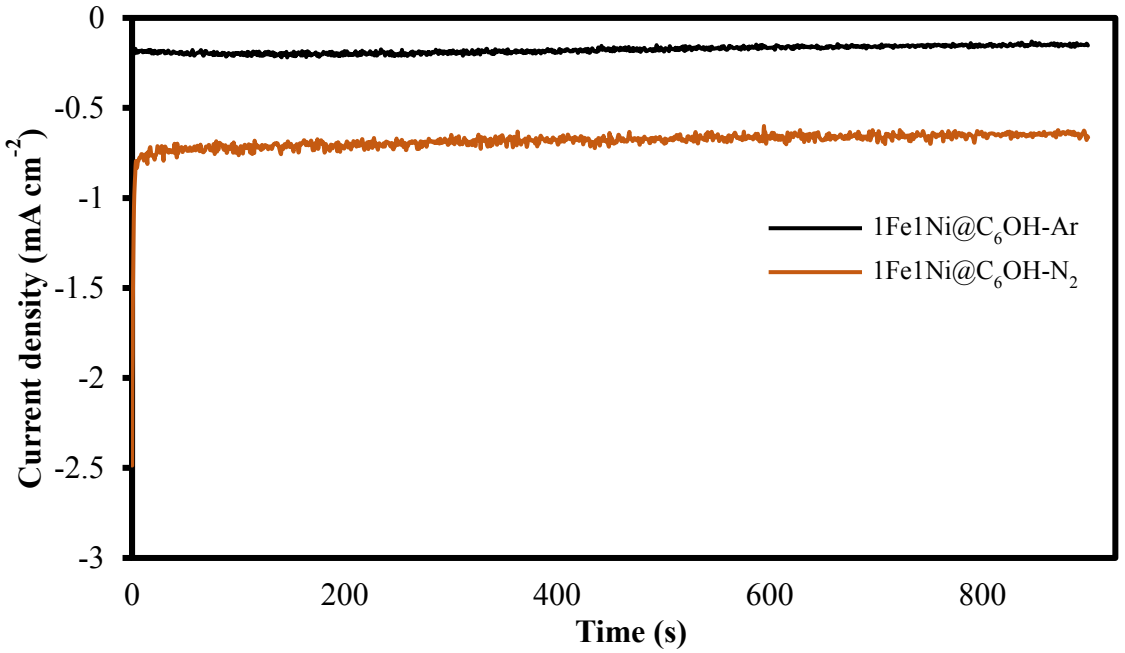

Figure 8. Chronoamperogram of 1Fe1Ni C_6OH functionalized films in 0.1 M phosphate solution under a nitrogen and argon atmosphere.

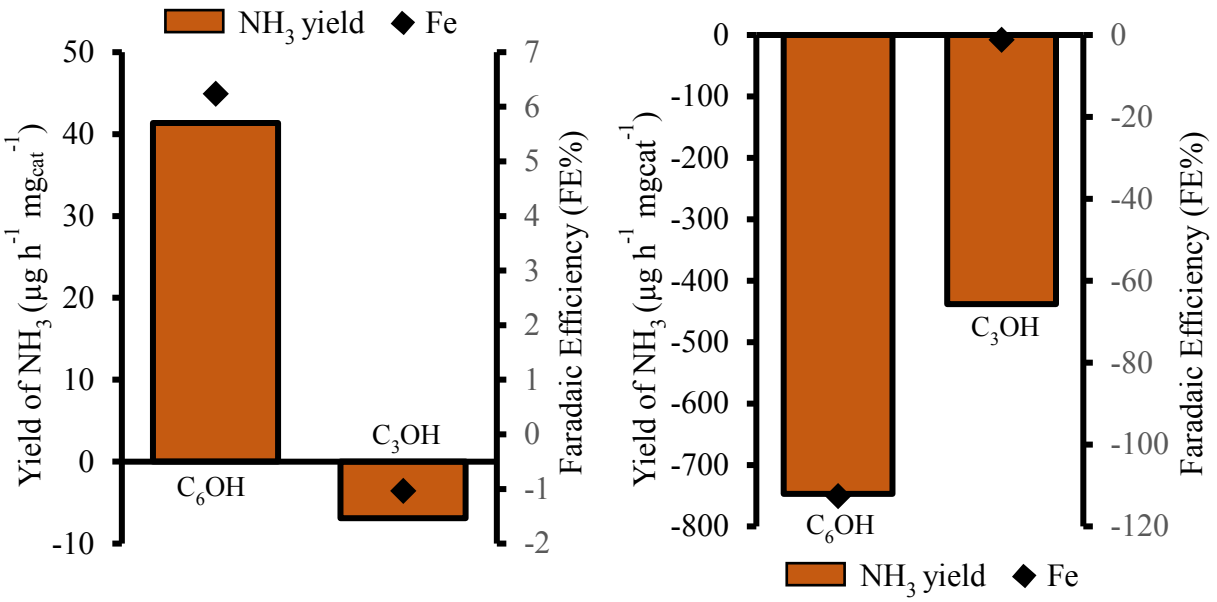

Figure 9. Rate of ammonia formation and FE in (a) in acid trap and (b) 0.1 M phosphate solution.

4. Conclusions

In summary, 0Fe1Ni, 1Fe0Ni, and 1Fe1Ni were successfully electrodeposited onto the quartz crystal to create a surface for C_3OH and C_6OH to be absorbed. C_6OH was shown to be stable on the surfaces of the all three composites with 1Fe1Ni having the best success. C_3OH was able to absorb to the surface of the films, however, they proved to be unstable and were easily washed off with ethanol. To improve absorption a second ligand with dual affinity for iron and sulfur should be attached to the surface of the film first before the thiol.

Electrochemical tests were performed only on the 1Fe1Ni film for NH_3 yield. The rate of NH_3 yield was 41.3 $\mu g\ h^{-1}\ mg_{cat.}^{-1}$ and the Faradic efficiency was 6.20% at -0.935 V (vs. RHE) at room temperature and ambient pressure in 0.1M phosphate solution with the 1Fe1Ni film functionalized with C_6OH. The C_3OH functionalized film proved to produce no ammonia. I believe that this work shows promise for functionalizing Fe-Ni bimetallic composites with thiols to improve ammonia production and Faradic efficiency. To improve the results a H-shaped electrochemical cell should be used to separate the chemistry between the cathode and the anode. Additionally, a better absorption method to attach thiols to the surface of the films should be used to improve the stabilization of the thiols.

References

1. **Giddey, S., et. al.,** "Review of electrochemical ammonia production technologies and materials", *International Journal of Hydrogen Energy*, **38,** pp. 14576-14594 (2013).

2. **Kyriakou, V., et. al.,** "Progress in the electrochemical synthesis of ammonia", *Catalysis Today*, **286,** pp. 2-13 (2017).

3. **Shipman, M. A., and Symes, M. D.,** "Recent progress towards the electrosynthesis of ammonia from sustainable resources", *Catalysis Today*, **286,** pp. 57-68 (2017).

4. **Smil, V.,** "Global population and nitrogen cycle", *Scientific America*, **277,** pp. 76-81 (1997).

5. **Liu, H.,** "Ammonia synthesis catalyst 100 years: Practice, enlightenment and challenge", *Chinese Journal of Catalysis*, **35,** pp. 1619-1640 (2014).

6. **Ertl, G.,** "Primary steps in catalytic synthesis of ammonia", *Journal of vacuum Science & Technology,* **1,** pp. 1247-1253 (1983).

7. **Ertl, G.,** "Reactions at surfaces: from atoms to complexity", *Angewandte Chemie,* **47,** pp. 3525-3535 (2008).

8. **Montoya, J. H.,** "The challenge of electrochemical ammonia synthesis: A new perspective on the role of nitrogen scaling relations", *Chemistry & Sustainability* **8,** pp. 2180-2186 (2015).

9. **Tanabe, Y., and Nishibayashi, Y.,** "Developing more sustainable processes for ammonia synthesis", *Coordination Chemistry Reviews,* **257,** pp. 853-858 (2013).

10. **Čorić, I., and Holland, P. L.,** "Insight into the iron-molybdenum cofactor of nitrogenase from synthetic iron complexes with sulfur, carbon, and hydride ligands

11. **Hoffman, B. M., et. al,** "Mechanism of nitrogen fixation by nitrogenase: The next stage", *Chemical Reviews,* **114,** pp. 4041-4062 (2014)

12. **Burgess, K. B., and Lowe, D. J.,** "Mechanism of molybdenum nitrogenase", *Chemical Reviews*, **96,** pp. 2983-3011 (1996).

13. **Erisman, J. W., et. al.,** "Reduced nitrogen in ecology and the environment", *Environmental Pollution*, **150,** pp. 140-149 (2007).

14. **Amar, I. A., et al.,** "Solid-state electrochemical synthesis of ammonia: A review", *Journal of Solid State Electrochemistry,* **15,** pp.1846-1860 (2011)

15. **Foster, S. L., et al.,** "Catalysts for nitrogen reduction to ammonia", *Nature Catalysis*, **1,** pp. 490-500 (2018).

16. **Liu, J., et. al.,** "Nitrogenase-mimic iron-containing chalcogels for photochemical reduction of dinitrogen to ammonia", *PNAS*, **113,** pp. 5530-5535 (2016).

17. **Skùlason, E., et. al.,** "A theoretical evaluation of possible transition metal electro-catalysts for N_2 reduction", *Physical Chemistry Chemical Physics*, **14,** pp. 1235-1245 (2012).

18. **Magistrato, A., et. al.,** "Nitrogen fixation by a molybdenum catalyst mimicking the function of the nitrogenase enzyme: A critical evaluation of DFT and solvent effects" , *Journal of Chemical Theory and Computation*, **3,** pp. 1708-1720 (2007).

19. **Čoriċ, I., and Holland, P. L.,** "Insight into the iron-molybdenum cofactor of nitrogenase from synthetic iron complexes with sulfur, carbon, and hydride ligands

20. **Marshall, S. T., et. al.,** "Controlled selectivity for palladium catalysts using self-assembled monolayers", *Nature Materials*, **9,** pp. 853-858 (2010).

21. **Chen, S., et al.,** "Room-temperature electrocatalytic synthesis of NH_3 from H_2O and N_2 in a gas-liquid-solid three-phase reactor", *ACS Sustainability Chemical Engineering,* **5,** pp. 7393-7400 (2017).

22. **Kong, J., et al.,** "Electrochemical synthesis of NH_3 at low temperature and atmospheric pressure using a γ -Fe2O3 catalyst", *ACS Sustainability Chemical Engineering,* **5,** pp/ 10986-10995 (2017).

6. Appendix

6.1 Cleaning of Au QCM Sensor

For efficient removal of organic and biological material on the surface of the QCM sensors the following protocol was followed. The entire procedure should be done with standard personal protective equipment under the hood. First, treat the sensors with UV/ozone for 10 minutes. Then prepare a 5:1:1 mixture of fresh ammonium peroxide solution (milliQ water, 25% ammonia, and 30% hydrogen peroxide) and heat the mixture to 75 ^{o}C. Allow the sensor to be immersed for five minutes then removed the sensor immediately and rinse with large amounts of water. The sensor was then dried with nitrogen gas and treated with UV/ozone for 10 minutes.